JOURNAL OF CATALYSIS 147, 57–71 (1994)

Molybdenum-oxo Species Deposited on Alumina by Adsorption

III. Advances in the Mechanism of $Mo^{(VI)}$ Deposition

N. Spanos and A. Lycourghiotis[1]

Department of Chemistry and the Institute of Chemical Engineering and Chemical Processes at High Temperatures, P.O. Box 1414, University Campus, GR-26500, Patras, Greece

Received June 18, 1993; revised November 29, 1993

The refinement of the mechanism of $Mo^{(VI)}$ deposition (proposed previously) from aqueous solutions on the γ-alumina surface by investigating critical mechanistic points is the subject of the present work. A mechanistic model involving the adsorption of $Mo_7O_{24}^{6-}$ and MoO_4^{2-} ions on sites created by the protonated surface hydroxyls of γ-alumina in the inner Helmholtz plane (IHP) of the double layer developed between the surface of the γ-alumina particles and the molybdate solutions, as well as the deposition of the MoO_4^{2-} ions through surface reaction with the neutral surface hydroxyls has been developed; it has been tested over a wide range of impregnation parameters (pH = 8.5–4.1 at 25°C, temperature 25–50°C at pH = 5 and doping of the carrier with various amounts of Na^+ and Li^+ ions). The testing of the model included the derivation of various equations corresponding to the model deposition equilibria, the calculation of the amount of the deposited Mo, of the difference in the isotherms of the hydrogen adsorption in presence and absence of molybdates, and of the ζ-potential of the γ-alumina particles in the molybdate solution (using an interactive code for the calculation of chemical equilibria in aqueous systems called SURFEQL), and the comparison of these parameters with the corresponding ones determined experimentally. The agreement between the calculated and experimentally determined parameters over a wide range of impregnating conditions allowed us to shed more light on the mechanism of the Mo deposition.

It was established that both the adsorption of $Mo_7O_{24}^{6-}$ and MoO_4^{2-} ions and the deposition of MoO_4^{2-} ions by surface reaction with two neutral hydroxyls of the support take place, but the contribution of each of these processes depends on the impregnating conditions. Specifically, in the pH range 8.5–6.1 the deposition practically occurs through the reaction of MoO_4^{2-} ions with neutral surface hydroxyls of the support resulting in the formation of the surface complex 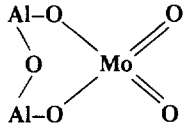 whereas at pH = 5 the adsorption of $Mo_7O_{24}^{6-}$ and MoO_4^{2-} ions is predominant and at pH = 4.1 the adsorption of $Mo_7O_{24}^{6-}$ ions prevails. Increasing the impregnating temperature, at pH = 5, from 25 to 50°C increases considerably the adsorption of $Mo_7O_{24}^{6-}$ ions and decreases further the deposition of MoO_4^{2-} ions by surface reaction, whereas it does not change considerably the extent of adsorption of MoO_4^{2-} ions. Finally, the doping with Li^+ and Na^+ ions increases both the extent of adsorption of $Mo_7O_{24}^{6-}$ ions and the extent of MoO_4^{2-} deposition by surface reaction, whereas it does not change considerably the extent of adsorption of MoO_4^{2-} ions. Moreover, it was demonstrated that each protonated surface hydroxyl creates one adsorption site and that strong lateral interactions are exerted between the deposited species, mainly between the adsorbed MoO_4^{2-} and $Mo_7O_{24}^{6-}$ ions, through water molecules located at the IHP. On the other hand, comparison of the adsorption constant with the reaction constant demonstrated that the ionic sorptive band is much stronger than the covalent Al–O–Mo bonds on the above-mentioned surface complex. Finally, the fact that the ratio $[MoO_4^{2-}]_b/[Mo_7O_{24}^{6-}]_b$ calculated in the bulk solution was always lower than the ratio $[MoO_4^{2-}]_{adsorb+react}/[Mo_7O_{24}^{6-}]_{adsorb}$ calculated in the deposited state corroborated the finding reported previously that, concerning deposition, the selectivity of the support surface for the MoO_4^{2-} ions is higher than the selectivity for the $Mo_7O_{24}^{6-}$ ions.

INTRODUCTION

In the first paper of this series (1) we attempted to clarify the mechanism of deposition of the molybdenum-oxo species on the γ-alumina surface during the application of the equilibrium adsorption technique.

Comparison of the adsorption data with the surface concentrations of neutral and protonated surface hydroxyls of the γ-alumina regulated by changing the temperature (2) or pH (2–5) of the impregnating suspension and doping the carrier (4, 5) allowed us to investigate the nature of the surface hydroxyls which are responsible for the creation of the depositing sites. This comparison strongly suggested that the groups responsible for the creation of the aforementioned sites are mainly the protonated surface hydroxyls. This conclusion was corroborated by a significant body of additional results presented in the second paper of this series (6), dealing with the

[1] To whom correspondence should be addressed.

0021-9517/94 $6.00

correlation of the protonated and neutral surface hydroxyls with the adsorption capacity of the support determined under various conditions. However, the observation that the values of the surface concentration of the adsorbed $Mo^{(VI)}$ were, in many cases, higher than those obtained for the corresponding values of the concentration of the protonated surface hydroxyls (Figs. 6, 7a, and 8 of Ref. (6)) implied that the participation of the neutral hydroxyls in the whole deposition cannot be precluded.

The combined use of potentiometric titrations and microelectrophoresis provided strong, though qualitative, evidence that the adsorbed molybdenum-oxo species were located in the inner Helmholtz plane (IHP) of the double layer developed between the surface of the γ-alumina particle and the molybdate solution. The theoretical analysis of the adsorption isotherms obtained experimentally, by deriving and testing several equations, allowed us on the one hand to confirm quantitatively the aforementioned qualitative evidences and on the other hand to demonstrate that the adsorption sites created in the IHP are energetically equivalent and that strong lateral interactions were exerted between the adsorbed $Mo^{(VI)}$ species through water molecules also adsorbed in the IHP.

Although the theoretical analysis of the adsorption isotherms and the combined use of the potentiometric titrations and microelectrophoresis allowed us to shed light on the mechanism of the deposition of the molybdenum-oxo species on the γ-alumina surface, we were not able to investigate in depth two important mechanistic points: (i) How important the participation of the neutral surface hydroxyls to the whole deposition mechanism is. Several authors in the past (7–11) were inclined to believe that the deposition of the molybdenum-oxo species took place by reaction of the MoO_4^{2-} ions with the neutral surface hydroxyls, whereas others (12–16) supported the view that the protonated surface hydroxyls are involved in the adsorption of the MoO_4^{2-} and/or $Mo_7O_{24}^{6-}$ ions, which exist in the impregnating solution almost exclusively under the conditions of impregnation. In our work (1) we showed that the adsorption is the principal mechanism of the MoO_4^{2-} or $Mo_7O_{24}^{6-}$ deposition, though it was noted that the participation of the neutral surface hydroxyls cannot be precluded. (ii) The analysis of the isotherms did not allow us to determine whether polymolybdates, principally $Mo_7O_{24}^{6-}$, are dissociated into MoO_4^{2-} before adsorbing (7, 9, 11, 16–19) or whether they are adsorbed intact (12, 13, 20–22), although it was necessary to assume that the MoO_4^{2-} ions are adsorbed more easily than the $Mo_7O_{24}^{6-}$ ions in order to explain the influence of adsorption and $Mo^{(VI)}$ concentration on the pH of the impregnating solutions.

The elucidation of the above-mentioned very important mechanistic points and the refinement of the mechanism proposed in the first paper of this series are the goal of the present work. Specifically, we tried to calculate under various conditions (temperature and pH of the impregnating solutions, doping of the carrier) the amount of the deposited $Mo^{(VI)}$ via reaction of the MoO_4^{2-} ions with the neutral surface hydroxyls resulting in the formation of

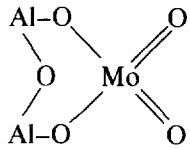

on the support surface; we also tried to investigate whether lateral interactions between the so-formed surface $Mo^{(VI)}$ species are exerted. Moreover, we tried to calculate, under the aforementioned conditions, the amount of $Mo^{(VI)}$ deposited via adsorption of the species MoO_4^{2-} and MoO_{24}^{6-}, separately, on sites created by the protonated surface hydroxyls in the IHP. Moreover, we attempted to elucidate the stoichiometry of the adsorption, investigating whether each adsorption site corresponds to one or two surface hydroxyls.

To do the above we adopted the following procedure. First, we write down a very probable mechanistic model based on the findings reported in the first paper of this series. This model incorporated all the eventualities for the deposition stated above (i.e., deposition via reaction and adsorption of different Mo species with different stoichiometries). Second, we derive several equations corresponding to the various deposition equilibria involved in the model. Third, we apply a computer program called SURFEQL (23) to the aforementioned model. This is an interactive code for calculating chemical equilibria in aqueous systems. Using this program we may calculate at 25°C the equilibrium concentrations of various species being either in the bulk solutions or in the solid/liquid interface. Finally, the calculated isotherms for the deposition of $Mo^{(VI)}$ under various conditions, the calculated difference in the isotherms of hydrogen adsorption on the γ-alumina surface in the presence and absence of molybdate ions as well as the calculated variation with pH of the potential at the OHP (Ψ_d) being almost equal to the potential at the shear plane (ζ-potential) are compared with the corresponding experimental curves. Thus, the validity of the proposed deposition model may be tested.

Most of the experimental data used in this paper have been taken from our previous work presented in the first paper of this series. The widely accepted triple-layer model for the double layer is implied in the present study (see, for example, Fig. 6 of Ref. (1)).

THEORETICAL CONSIDERATIONS

Deposition Model

In light of our findings reported in first and second paper of this series and according to the literature (7–22,

24) we propose the following quite general deposition model:

$$AlOH_2^+ + MoO_4^{2-} \overset{K_1}{\rightleftarrows} AlOH_2^+ \ldots MoO_4^{2-} \quad [1a]$$

$$2AlOH_2^+ + MoO_4^{2-} \overset{K_2}{\rightleftarrows} (AlOH_2^+)_2 \ldots MoO_4^{2-} \quad [1b]$$

$$AlOH_2^+ + Mo_7O_{24}^{6-} \overset{K_3}{\rightleftarrows} AlOH_2^+ \ldots Mo_7O_{24}^{6-} \quad [1c]$$

$$2AlOH_2^+ + Mo_7O_{24}^{6-} \overset{K_4}{\rightleftarrows} (AlOH_2^+)_2 \ldots Mo_7O_{24}^{6-} \quad [1d]$$

$$2AlOH + MoO_4^{2-} \overset{K_5}{\rightleftarrows} \begin{matrix} Al\text{-}O & & O \\ & O\quad Mo & \\ Al\text{-}O & & O \end{matrix} + 2OH^- . \quad [1e]$$

According to this model the monomeric species, MoO_4^{2-}, being in the IHP [plane 1], is adsorbed on a site in this place created by one or two protonated surface hydroxyls ($AlOH_2^+$) being on the surface [plane 0] and provides respectively the adsorbed species illustrated in equilibria [1a] and [1b]. The r.h.s. part of these species is located in the IHP, whereas the l.h.s. part of these species is on the support surface. Similarly equilibria [1c] and [1d] describe the adsorption of the $Mo_7O_{24}^{6-}$ ions, being in the IHP, on a site created in this plane by one or two protonated surface hydroxyls. Finally, according to the model, the deposition of the MoO_4^{2-}, being in the IHP, may take place by reacting with two neutral surface hydroxyls, resulting in the formation of the surface species illustrated in equilibrium [1e]. It should be noted that according to the proposed model strong lateral interactions are exerted between the deposited species, mainly between the adsorbed MoO_4^{2-} and $Mo_7O_{24}^{6-}$ ions, through water molecules located at the IHP.

It is obvious that the formation constants of the surface [1e] and sorptive [1a]–[1d] complexes illustrated in equilibria [1] are given by

$$K_{f,1} = [AlOH_2^+ \ldots MoO_4^{2-}]/[AlOH_2^+][MoO_4^{2-}] \quad [2a]$$

$$K_{f,2} = [(AlOH_2^+)_2 \ldots MoO_4^{2-}]/[AlOH_2^+]^2[MoO_4^{2-}] \quad [2b]$$

$$K_{f,3} = [AlOH_2^+ \ldots Mo_7O_{24}^{6-}]/[AlOH_2^+][Mo_7O_{24}^{6-}] \quad [2c]$$

$$K_{f,4} = [(AlOH_2^+)_2 \ldots Mo_7O_{24}^{6-}]/[AlOH_2^+]^2[Mo_7O_{24}^{6-}] \quad [2d]$$

$$K_{f,5} = [Al_2MoO_4][OH^-]^2/[AlOH]^2[MoO_4^{2-}]. \quad [2e]$$

Derivation of the Model Equations

Let us begin with the adsorption of the MoO_4^{2-} described by Eq. [1a]. The following equations provide the electrochemical potentials of the species involved in equilibrium [1a] (1, 25):

$$\tilde{\mu}_1 = \mu_1^0 + RT \ln[MoO_4^{2-}]_1 + Z_1F\varphi_1 \quad [3a]$$

$$\tilde{\mu}_2 = \mu_2^0 + RT \ln(1 - \theta) + Z_2F\varphi_0 \quad [3b]$$

$$\tilde{\mu}_3 = \mu_3^0 + RT \ln \theta_1 + Z_1F\varphi_1. \quad [3c]$$

Here, $\tilde{\mu}_1$, $\tilde{\mu}_2$, $\tilde{\mu}_3$, μ_1^0, μ_2^0, and μ_3^0 represent the electrochemical potentials and the corresponding standard state chemical potentials for the species MoO_4^{2-}, $AlOH_2^+$, and $AlOH_2^+ \ldots MoO_4^{2-}$, respectively. $[MoO_4^{2-}]_1$ is the concentration of MoO_4^{2-} ions in the IHP. Z_1 and Z_2 represent the charge of the species MoO_4^{2-} and $AlOH_2^+$, respectively. θ_1 and θ denote, respectively, the fraction of the sites covered by the $Mo^{(VI)}$ species illustrated in the r.h.s. of equilibrium [1a] and by the $Mo^{(VI)}$ species illustrated in the r.h.s. of equilibria [1a]–[1e]. Finally, φ_0 and φ_1 symbolize the Galvani potential on the surface and in the IHP, respectively. It should be noted here that, assuming no preferential coverage of the surface sites $AlOH_2^+$ and AlOH by the deposited $Mo^{(VI)}$ species, each of the fractions of the covered $AlOH_2^+$ and AlOH sites is approximately equal to the fraction of the covered total surface sites [$AlOH_2^+$ and AlOH]. Therefore, in Eq. [3b] the fraction of the free $AlOH_2^+$ sites may be replaced by the fraction of the free total sites, $1 - \theta$. According to equilibrium [1a]

$$\tilde{\mu}_1 + \tilde{\mu}_2 = \tilde{\mu}_3. \quad [4]$$

Substitution of Eqs. [3] into Eq. [4] yields

$$RT \ln\{\theta_1/(1 - \theta)\} = -\Delta G^\circ_{chem,1} + Z_2F\varphi_0 + RT \ln[MoO_4^{2-}]_1, \quad [5]$$

where $\Delta G^\circ_{chem,1} = \mu_3^0 - (\mu_1^0 + \mu_2^0)$ represents the contribution of the chemical interactions to the standard free energy of adsorption, $\Delta G^\circ_{ads,1}$, relative to equilibrium [1a]. The concentration of the MoO_4^{2-} ions in the IHP is related with its bulk concentration, $[MoO_4^{2-}]_b$, by

$$[MoO_4^{2-}]_1 = [MoO_4^{2-}]_b \exp(-Z_1F\Psi_1/RT), \quad [6]$$

where Ψ_1 represents the Volta potential at the IHP. Substitution of the $[MoO_4^{2-}]_1$ by its equal allows the transformation of Eq. [5] into

$$\theta_1/(1 - \theta) = \exp\{(-\Delta G^\circ_{chem,1} - \Delta G^\circ_{elect,1})/RT\}\,[MoO_4^{2-}]_b, \quad [7]$$

where $\Delta G^\circ_{elect,1}$ represents the contribution of the electrostatic interactions to the standard free energy of adsorp-

tion relative to equilibrium [1a]. In other words, the term $\Delta G^{\circ}_{elect,1}$ represents the work arising from the interactions of the species adsorbed according to the equilibrium [1a] with the electric field due to the charged surface. This is related with φ_0 and Ψ_1 by

$$\Delta G^{\circ}_{elect,1} = -F(2\Psi_1 + \varphi_0). \quad [8]$$

Following Hough and Rendall (26) and assuming that the magnitude of the lateral interactions between the adsorbed molybdate ions is practically independent from the kind of these ions we may write

$$\Delta G^{\circ}_{chem,1} = \Delta G^{\circ}_{cs,1} + \Delta G^{\circ}_{cc}, \quad [9]$$

where $\Delta G^{\circ}_{cs,1}$ and ΔG°_{cc} represent, respectively, the contribution to the $\Delta G^{\circ}_{chem,1}$ of the chemical interactions between the adsorbed MoO_4^{2-} ions and the support and those between the adsorbed MoO_4^{2-} ions. At this point it should be noted that the term ΔG°_{cc} involves the electrical lateral interactions besides the chemical ones. Assuming that $\Delta G^{\circ}_{cc} = -E\theta$ (27), where E is the energy of the lateral interactions, we obtain

$$\Delta G^{\circ}_{chem,1} = \Delta G^{\circ}_{cs,1} - E\theta. \quad [10]$$

Replacing θ by Γ/Γ_m, where Γ and Γ_m represent the total surface concentration of $Mo^{(VI)}$ determined experimentally and the corresponding monolayer concentration (1), Eq. [10] is transformed into

$$\Delta G^{\circ}_{chem,1} = \Delta G^{\circ}_{cs,1} - \lambda\Gamma, \quad [11]$$

where λ is a constant equal to E/Γ_m. Combining Eqs. [7] and [11] provides

$$\theta_1/(1-\theta) = K_1[MoO_4^{2-}]_b \exp(\lambda\Gamma/RT), \quad [12]$$

where $K_1 = \exp[(-\Delta G^{\circ}_{cs,1} - \Delta G^{\circ}_{elect,1})/RT]$ [13]

is the conditional adsorption constant of equilibrium [1a].

Following the above-described procedure we may easily derive

$$\theta_2/(1-\theta) = K_2[MoO_4^{2-}]_b \exp(\lambda\Gamma/RT) \quad [14]$$

$$\theta_3/(1-\theta) = K_3[Mo_7O_{24}^{6-}]_b \exp(\lambda\Gamma/RT) \quad [15]$$

$$\theta_4/(1-\theta) = K_4[Mo_7O_{24}^{6-}]_b \exp(\lambda\Gamma/RT), \quad [16]$$

which correspond to the equilibria [1b]–[1d], where θ_2, θ_3, and θ_4 represent, respectively, the fraction of the surface sites covered respectively by the Mo entities illustrated in the r.h.s. of the equilibria [1b], [1c], and [1d]. The constants K_i ($i = 2, 3, 4$) are given by

$$K_i = \exp\{(-\Delta G^{\circ}_{cs,i} - \Delta G^{\circ}_{elect,i})/RT\}. \quad [17]$$

The $\Delta G^{\circ}_{cs,i}$ and $\Delta G^{\circ}_{elect,i}$ represent, respectively, the contribution of the chemical (between the deposited species and the support) and electrostatic interactions to the standard free energies of equilibria [1b]–[1d]. $\Delta G^{\circ}_{elect,i}$ is equal to $-2F(\Psi_1 + \varphi_0)$, $-F(6\Psi_1 + \varphi_0)$, and $-2F(3\Psi_1 + \varphi_0)$ for $i = 2$, 3, and 4, respectively. At this point it should be noted that in the case of equilibria [1b] and [1d] the electrochemical potential of the $AlOH_2^+$ species was assumed to be expressed by

$$\tilde{\mu}_2 = \mu_2^0 + RT \ln(1-\theta)^{1/2} + Z_2F\varphi_0. \quad [18]$$

This assumption was made to take into account that the chemical potential of a $AlOH_2^+$ site adjacent with another $AlOH_2^+$ site should be higher compared with that of an isolated $AlOH_2^+$ site, which does not react according to equilibria [1b] and [1d].

Let us finally derive the model equations for equilibrium [1e]. The electrochemical potentials of the species involved in this equilibrium are given by the following equations:

$$\tilde{\mu}_1 = \mu_1^0 + RT \ln[MoO_4^{2-}]_1 + Z_1F\varphi_1 \quad [19a]$$

$$\tilde{\mu}_2 = \mu_2^0 + RT \ln(1-\theta)^{1/2} + Z_1F\varphi_0 \quad [19b]$$

$$\tilde{\mu}_3 = \mu_3^0 + RT \ln\theta_5 + Z_3F\varphi_1 \quad [19c]$$

$$\tilde{\mu}_4 = \mu_4^0 + RT \ln[OH^-]_0 + Z_4F\varphi_0 \quad [19d]$$

In the above equations $\tilde{\mu}_1$, $\tilde{\mu}_2$, $\tilde{\mu}_3$, $\tilde{\mu}_4$, μ_1^0, μ_2^0, μ_3^0, μ_4^0, Z_1, Z_2, Z_3, and Z_4 denote, respectively, the electrochemical potentials, the corresponding standard state chemical potentials, and the charges of the species MoO_4^{2-}, AlOH,

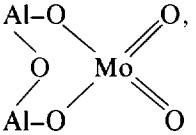

and OH^-. It is notable that $Z_1 = -2$, $Z_2 = 0$, $Z_3 = 0$, and $Z_4 = -1$. θ_5 denotes the fraction of the sites covered by the $Mo^{(VI)}$ species illustrated in the r.h.s. of equilibrium [1e]. φ_0 and φ_1 have the meaning stated before. The electrochemical potential of the AlOH species was assumed to be expressed by Eq. [19b] for the same reasons as in the case of the $AlOH_2^+$ species in Eq. [18]. Due to equilibrium [1e] we may write

$$\tilde{\mu}_1 + 2\tilde{\mu}_2 = \tilde{\mu}_3 + 2\tilde{\mu}_4. \quad [20]$$

The concentration of the OH^- ions released on the surface, $[OH^-]_0$, is related with its bulk concentration,

$[OH^-]_b$, by

$$[OH^-]_0 = [OH^-]_b \exp(-Z_4F\Psi_0/RT), \quad [21]$$

where Ψ_0 represents the Volta potential on the support surface. By combining Eq. [6] and Eqs. [19]–[21] we may easily obtain

$$\theta_5/(1-\theta) = \exp\{[-\Delta G^\circ_{chem,5} + 2F(\varphi_0 - \Psi_0) - 2F(\varphi_1 - \Psi_1)]/RT\}[MoO_4^{2-}]_b/[OH^-]_b^2, \quad [22]$$

where $\Delta G^\circ_{chem,5} = \mu_3^0 + 2\mu_4^0 - \mu_1^0 - 2\mu_2^0$. Since both differences $\varphi_0 - \Psi_0$ and $\varphi_1 - \Psi_1$ are equal to the inner potential, the electrostatic free energy, $\Delta G^\circ_{elect,5} = -2F(\varphi_0 - \Psi_0) + 2F(\varphi_1 - \Psi_1)$ is equal to zero. Therefore, following a procedure similar to that followed in the case of Eq. [7], and taking into account that $[OH^-]_b^2 = 10^{-(28-2pH)}$ results in

$$\theta_5/(1-\theta) = K_5[MoO_4^{2-}]_b \exp(\lambda\Gamma/RT), \quad [23]$$

where K_5 is the conditional adsorption constant of equilibrium [1e], given by

$$K_5 = \{\exp(-\Delta G^\circ_{cs,5}/RT)\}\, 10^{28-2pH}. \quad [24]$$

Inspection of Eq. [24] shows that K_5 is an apparent deposition constant because it involves the term 10^{28-2pH} (i.e., $[OH^-]_b^{-2}$). Therefore, the transformation of K_5 into an intrinsic constant for equilibrium [1e] may be performed as

$$K'_{f,5} = K_5\, 10^{-(28-2pH)} = \exp(-\Delta G^\circ_{cs,5}/RT). \quad [25]$$

Inspection of Eqs. [13], [17], [24], and [25] shows that the conditional adsorption constants K_1, K_2, K_3, K_4, and $K'_{f,5}$ do not involve the term ΔG°_{cc}, namely the contribution of the lateral interactions to the overall deposition process. Therefore, in order to calculate the formation constants illustrated in Eqs. [2] we may multiply the aforementioned constants with $\exp(\lambda\Gamma/RT)$.

From the above it can be observed that the values of the formation constants should change with the surface $Mo^{(VI)}$ concentration, Γ, and consequently with the equilibrium concentration, C_{eq}. A modification of the SURFEQL, made by us, allowed us to include this change in the calculated formation constants.

According to the model proposed above $\theta = \theta_1 + \theta_2 + \theta_3 + \theta_4 + \theta_5$. Therefore

$$\theta/(1-\theta) = \theta_1/(1-\theta) + \theta_2/(1-\theta) + \theta_3/(1-\theta) + \theta_4/(1-\theta) + \theta_5/(1-\theta). \quad [26]$$

Replacing the r.h.s. terms of Eq. [26] by the corresponding r.h.s. of Eqs. [12], [14]–[16], and [23] we obtain

$$\theta/(1-\theta) = (K_1[MoO_4^{2-}]_b + K_2[MoO_4^{2-}]_b + K_3[Mo_7O_{24}^{6-}]_b + K_4[Mo_7O_{24}^{6-}]_b + K_5[MoO_4^{2-}]_b)\exp(\lambda\Gamma/RT). \quad [27]$$

The concentration of the MoO_4^{2-} and $Mo_7O_{24}^{6-}$ ions in the bulk solution may be expressed as a function of the total equilibrium concentration, C_{eq} (mol $Mo^{(VI)}$ dm^{-3}), which is experimentally determined (1). Specifically, we have assumed (1) that $[MoO_4^{2-}]_b = \alpha_1 C_{eq}$ and $[Mo_7O_{24}^{6-}]_b = \alpha_2 C_{eq}$, where the coefficients α_1 and α_2 may be calculated at any pH value on the basis of the following equilibrium (28):

$$Mo_7O_{24}^{6-} + 4H_2O \overset{K'}{\rightleftarrows} 7MoO_4^{2-} + 8H^+. \quad [28]$$

Moreover, we assume that the values of conditional adsorption constants related with the adsorption equilibria (equilibria [1a]–[1d]) do not actually differ from one another ($K_1 \approx K_2 \approx K_3 \approx K_4$ and then $K_{f,1} \approx K_{f,2} \approx K_{f,3} \approx K_{f,4}$). Thus, Eq. [27] may be transformed into

$$\theta/(1-\theta) = \tilde{K} C_{eq} \exp(\lambda\Gamma/RT) \quad [29]$$

and then

$$1/\Gamma = 1/\Gamma_m + 1/\Gamma_m \tilde{K} C_{eq} \exp(\lambda\Gamma/RT), \quad [30]$$

where

$$\tilde{K} = 2(\alpha_1 + \alpha_2)K_1 + \alpha_1 K_5. \quad [31]$$

Comparison of Eq. [30] with Eq. [21] of Ref. (1) reveals that these equations are formalistically identical. At this point it should be mentioned that the deposition isotherms obtained in the work presenetd in Refs. (1) and (6) had been successfully analyzed using this equation and that the determination of $\tilde{K}$ and λ values under various conditions had been attained. The values of $\tilde{K}$ are used in the present work in order to calculate the values of K_1 (K_5) by guessing proper values for K_5 (K_1) (see Eq. [31]) which allow a fitting of the calculated deposition isotherms with the adsorption data.

Application of the SURFEQL

Tables 1 and 2 show, respectively, the parameters required for and the parameters or variables derived from the application of SURFEQL to the proposed model.

Parameters K_1^{int} and K_2^{int} illustrated in Table 1 denote, respectively, the deprotonation constants of the positive

TABLE 1

Compilation of Parameters Required for the Application of SURFEQL to the Proposed Model

Parameter	Symbol	Value	Units	Reference
Total surface sites density	N_s	8	sites nm^{-2}	(29, 30)
Deprotonation constant of $AlOH_2^+$	K_1^{int}			(1, 2, 4, 5)
Deprotonation constant of AlOH	K_2^{int}			(1, 2, 4, 5)
Constant of equilibrium (28)	K'	$10^{-52.81}$		(28)
Adsorption constant	$\hat{K}$			(1, Eq. [21])
Conditional constant of adsorption through electrostatic forces	K_1			Guess (see text, page 14)
Conditional constant of adsorption through chemical reaction	K_s			Determined from Eq. [31]
Ratio of MoO_4^{2-} ($Mo_7O_{24}^{6-}$) ion concentration to the total $Mo^{(VI)}$ concentration in the bulk solution	α_1 (α_2)			Calculated on the basis of Eq. [28]
Energy of the lateral interactions	E		kJ mol^{-1}	(1, 6)
Total $Mo^{(VI)}$ concentration	$[Mo^{(VI)}]_t$		mol dm^{-3}	(1, 6)
Total NH_4^+ concentration	$[NH_4^+]_t$		mol dm^{-3}	(1, 6)
Total NO_3^- concentration	$[NO_3^-]_t$		mol dm^{-3}	(1, 6)
pH	pH			(1, 6)
Specific surface area	SSA	123	m^2 g^{-1}	(1, 6)
Solid concentration	SC	3.57	g dm^{-3}	(1, 6)
Ionic strength	I	0.1	mol dm^{-3}	(1, 6)
Inner capacitance	C_1	110	F m^{-2}	(1, Fig. 6)
Outer capacitance	C_2	0.2	F m^{-2}	(1, Fig. 6)

TABLE 2

Compilation of Parameters or Variables Derived from the Application of SURFEQL to the Proposed Model

Parameter	Symbol	Units
Surface charge density	σ_0	C m^{-2}
Charge density at the IHP	σ_1	C m^{-2}
Charge density at the OHP	σ_d	C m^{-2}
Surface potential	Ψ_0	V
Potential at the IHP	Ψ_1	V
Potential at the OHP	Ψ_d	V
Equilibrium concentration of H^+	$[H^+]$	mol dm^{-3}
Equilibrium concentration of MoO_4^{-2}	$[MoO_4^{2-}]$	mol dm^{-3}
Equilibrium concentration of $Mo_7O_{24}^{6-}$	$[Mo_7O_{24}^{6-}]$	mol dm^{-3}
Equilibrium concentration of $HMoO_4^-$	$[HMoO_4^-]$	mol dm^{-3}
Equilibrium concentration of NH_4^+	$[NH_4^+]$	mol dm^{-3}
Equilibrium concentration of NO_3^-	$[No_3^-]$	mol dm^{-3}
Equilibrium concentration of $AlOH_2^+ \ldots MoO_4^{2-}$	$[AlOH_2^+ \ldots MoO_4^{2-}]$	mol dm^{-3}
Equilibrium concentration of $(AlOH_2^+)_2 \ldots MoO_4^{2-}$	$[(AlOH_2^+)_2 \ldots MoO_4^{2-}]$	mol dm^{-3}
Equilibrium concentration of $AlOH_2^+ \ldots Mo_7O_{24}^{6-}$	$[AlOH_2^+ \ldots Mo_7O_{24}^{6-}]$	mol dm^{-3}
Equilibrium concentration of $(AlOH_2^+)_2 \ldots Mo_7O_{24}^{6-}$	$[(AlOH_2^+)_2 \ldots Mo_7O_{24}^{6-}]$	mol dm^{-3}
Equilibrium concentration of Al_2MoO_4	$[Al_2MoO_4]$	mol dm^{-3}
Equilibrium concentration of AlOH	[AlOH]	mol dm^{-3}
Equilibrium concentration of $AlOH_2^+$	$[AlOH_2^+]$	mol dm^{-3}
Equilibrium concentration of AlO^-	$[AlO^-]$	mol dm^{-3}

and neutral surface hydroxyls following the well-established surface ionization model described by

$$AlOH_2^+ \overset{K_1^{int}}{\rightleftharpoons} AlOH + H_s^+ \quad [32a]$$

$$AlOH \overset{K_2^{int}}{\rightleftharpoons} AlO^- + H_s^+ \quad [32b]$$

$$H_s^+ \rightleftharpoons H_b^+ \quad [32c]$$

$$H_2O \rightleftharpoons H_b^+ + OH_b^-, \quad [32d]$$

where b and s denote, respectively, the bulk solution and the support surface.

The values of the above constants do not change due to the presence of the molybdenum-oxo species in the electrolyte suspension. Therefore, we used their values determined by us in the absence of the aforementioned species (1, 2, 4, 5). As illustrated in Table 2, the application of SURFEQL may result in the calculation of the surface concentration of the groups depicted above in the presence and absence of the molybdenum-oxo species.

RESULTS AND DISCUSSION

Test of the Proposed Model

We attempt to test the validity of the proposed model in three ways.

First, we compare the calculated surface concentration, Γ, with the experimental one under various conditions (adsorption of the MoO_4^{2-} and $Mo_7O_{24}^{6-}$ ions on the surface of pure and Na^+ or Li^+-doped γ-alumina over a pH range between 4.0 and 8.5 and temperatures ranging from 25 to 50°C) (6).

Second, we study the difference between the hydrogen ions consumed for the protonation of the deprotonated and neutral surface hydroxyls (see equilibria [32]) in the presence and absence of the molybdenum-oxo species. This difference, $\Delta H^+_{consumed}$, may be determined experimentally using the method of the potentiometric titrations. Details concerning its determination in various systems have been reported elsewhere (31–33). Moreover, this difference may be calculated using SURFEQL. In fact, the application of this program allows the calculation of the difference between "the total protonated minus total deprotonated surface hydroxyls" in the presence and absence of the molybdenum-oxo species, $\Delta(AlOH_2^+\text{-}AlO^-)_t$. Comparison of the experimental with the calculated difference mentioned above offers another methodology for testing the model.

Both of the above-mentioned methods are based on the ability of the γ-alumina surface to react with MoO_4^{2-} and H^+ ions or to adsorb MoO_4^{2-} and $Mo_7O_{24}^{6-}$ ions in the IHP. Moreover, these processes are responsible for the ob-

served change of the charge and thus of the potential at the shear plane of the double layer, ζ-potential (Fig. 6 of Ref. (1)), caused by the presence of the molybdenum-oxo species in the electrolyte solution (Fig. 5 of Ref. (1)). The negative value of ζ-potential in the presence of the aforementioned species over a wide pH range corroborated the view that the adsorbed MoO_4^{2-} and $Mo_7O_{24}^{6-}$ ions are located in the IHP (1). Now the comparison of the ζ-potential values determined in the presence of oxo-molybdenum species over a wide pH range with the corresponding ones predicted by the proposed mechanistic model offers a third completely independent methodology for testing the model.

At this point it should be mentioned that in the cases where work at temperatures other than 25°C was required, SURFEQL was properly amended.

In Figs. 1–13 the deposition isotherms determined experimentally (curve a, □) and the corresponding isotherms calculated by applying SURFEQL to the proposed model (curve a, △) are illustrated. It can be observed that in all cases a very good agreement between experimental and model curves is achieved. The fact that this very good agreement is obtained at 25°C and various pHs (Figs. 1–5), at pH = 5 and various impregnating temperatures (Figs. 1, 6–8), or after doping by Na^+ (Figs. 9–11) or Li^+ (Figs. 12, 13) demonstrates the validity of the proposed model over a wide range of the impregnation parameters. It should be noted here that there is one and only one set of K_1 and K_5 values satisfying Eq. [31] which provides

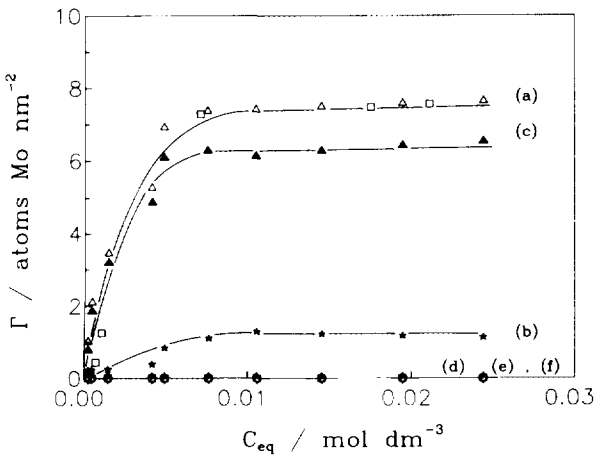

FIG. 1. Variation of the surface concentration of $Mo^{(VI)}$ with equilibrium $Mo^{(VI)}$ concentration: (a) (□) experimental and (△) calculated isotherm for the total Mo deposition. Calculated isotherms for the $Mo^{(VI)}$ deposition (b) through adsorption of one MoO_4^{2-} ion per site created by one $AlOH_2^+$ group, (c) through adsorption of one $Mo_7O_{24}^{6-}$ ion per site created by one $AlOH_2^+$ group, (d) through reaction of one MoO_4^{2-} ion with two neutral surface hydroxyls, and through adsorption (e) of one MoO_4^{2-} ion per site created by two $AlOH_2^+$ groups and (f) of one $Mo_7O_{24}^{6-}$ ion per site created by two $AlOH_2^+$ groups. Deposition on pure γ-alumina, pH = 4.1, temperature = 25°C, ionic strength = 0.1 *M* NH_4NO_3.

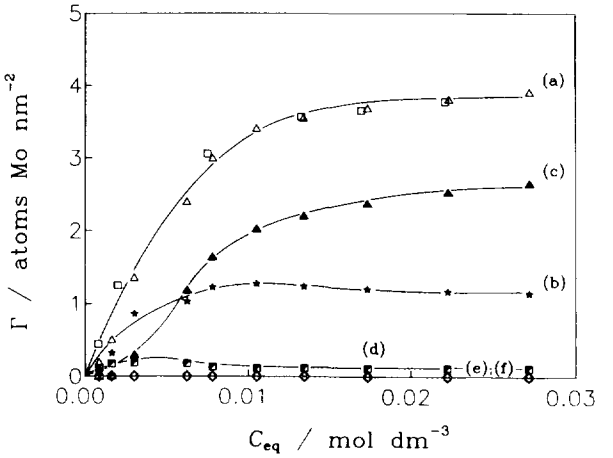

FIG. 2. Variation of the surface concentration of $Mo^{(VI)}$ with equilibrium $Mo^{(VI)}$ concentration. Deposition on pure γ-alumina, pH = 5.0, temperature = 25°C, ionic strength = 0.1 *M* NH_4NO_3. Symbols as in Fig. 1.

this very good agreement. Concerning the energy of the lateral interactions it was necessary to assume that this energy between $Mo_7O_{24}^{6-}$ ions is threefold of that between MoO_4^{2-} ions. This assumption seems reasonable due to the relationship between the valences of these ions, provided that the lateral interactions are mainly electrostatic as mentioned before.

Figure 14 illustrates the variations, with pH, of the differences in the presence and absence of molybdenum-oxo species, of the hydrogen consumed on the surface of the support, $\Delta H^+_{consumed}$ (curve a), and of the "total protonated minus total deprotonated surface hydroxyls," $\Delta(AlOH_2^+\text{-}AlO^-)_t$ (curve b). The very good agreement between curves a and b corroborates the mechanistic model proposed in the present study.

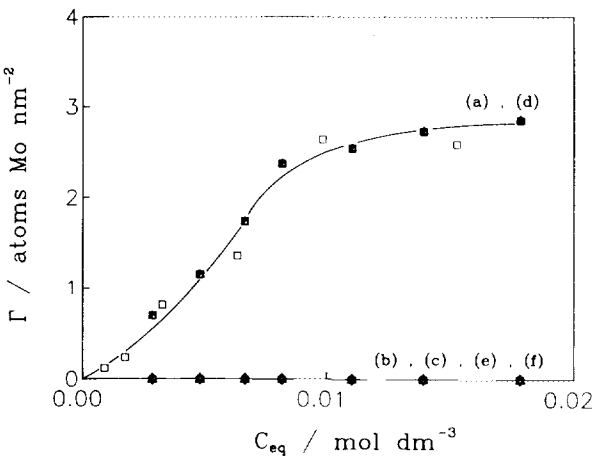

FIG. 3. Variation of the surface concentration of $Mo^{(VI)}$ with equilibrium $Mo^{(VI)}$ concentration. Deposition on pure γ-alumina, pH = 6.1, temperature = 25°C, ionic strength = 0.1 *M* NH_4NO_3. Symbols as in Fig. 1.

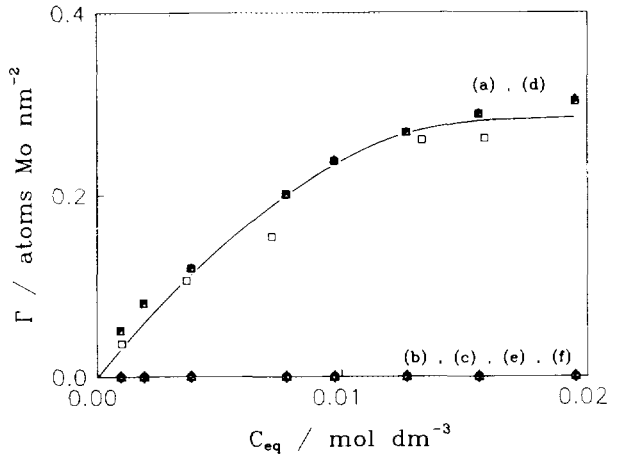

FIG. 4. Variation of the surface concentration of $Mo^{(VI)}$ with equilibrium $Mo^{(VI)}$ concentration. Deposition on pure γ-alumina, pH = 7.3, temperature = 25°C, ionic strength = 0.1 *M* NH_4NO_3. Symbols as in Fig. 1.

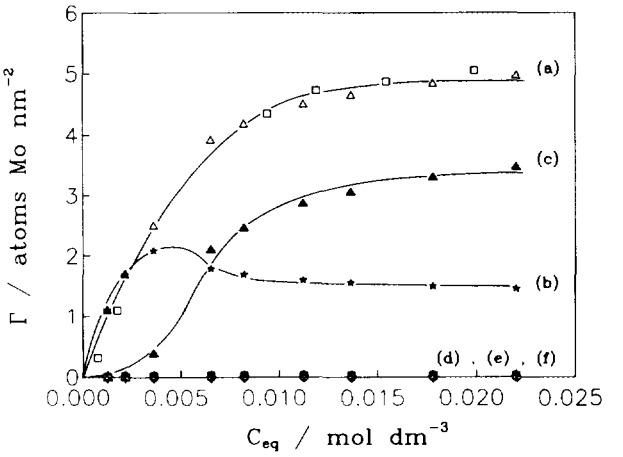

FIG. 6. Variation of the surface concentration of $Mo^{(VI)}$ with equilibrium $Mo^{(VI)}$ concentration. Deposition on pure γ-alumina, pH = 5.0, temperature = 35°C, ionic strength = 0.1 *M* NH_4NO_3. Symbols as in Fig. 1.

Figure 15 illustrates the variation, with pH, of the ζ-potential determined using microelectrophoretic mobility data (curve a) as well as of the $\Psi_d \approx \zeta$-potential calculated using the deposition model proposed (curve b). The very good agreement between the experimental and model curves offers an additional strong support of the mechanism proposed.

Taking into account the previous discussion concerning the validity of the proposed mechanism of adsorption one might argue that the procedure followed involved the supersimplified assumption that the four adsorption constants K_1–K_4 take the same value. But this is not the case. In fact, Figs. 1–13 (curves e and f) clearly show that in all cases studied the adsorption of MoO_4^{2-} or $Mo_7O_{24}^{6-}$ ions on a site created by two protonated surface hydroxyls is negligible. This means that the equilibria [1a], [1c], and [1e] describe the deposition mechanism adequately. Thus, the actual assumption involved in the aforementioned procedure is that $K_1 \approx K_3$.

It should be noted that mechanisms involving *only* surface reaction (equilibrium [1e]), *only* adsorption (equilibria [1a] and [1c]), adsorption of x MoO_4^{2-} ions per site or adsorption of x $Mo_7O_{24}^{6-}$ ions per site ($x = 2, \ldots, 6$) have also been developed and tested following the aforementioned procedure, but no agreement has been attained between the experimental and calculated isotherms over the wide range of the impregnating condition examined in the present study.

A schematic representation of the deposition of the MoO_4^{2-} and $Mo_7O_{24}^{6-}$ ions on the γ-alumina surface

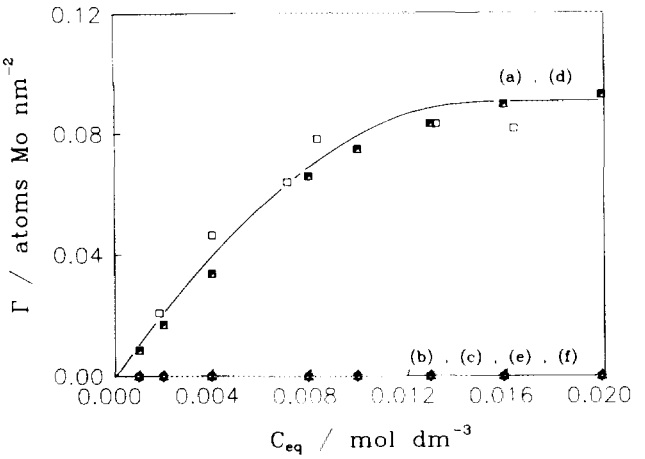

FIG. 5. Variation of the surface concentration of $Mo^{(VI)}$ with equilibrium $Mo^{(VI)}$ concentration. Deposition on pure γ-alumina, pH = 8.5, temperature = 25°C, ionic strength = 0.1 *M* NH_4NO_3. Symbols as in Fig. 1.

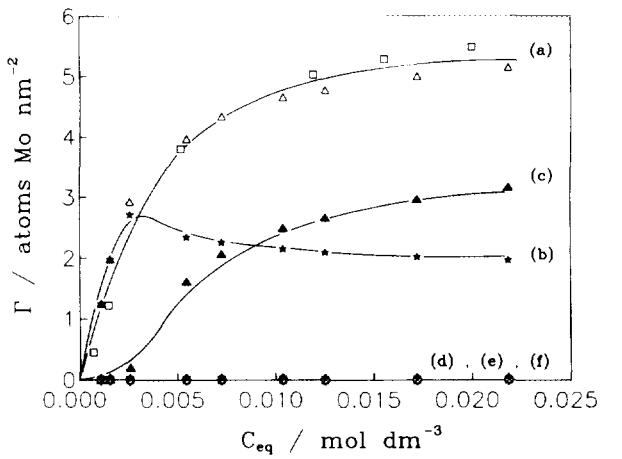

FIG. 7. Variation of the surface concentration of $Mo^{(VI)}$ with equilibrium $Mo^{(VI)}$ concentration. Deposition on pure γ-alumina, pH = 5.0, temperature = 40°C, ionic strength = 0.1 *M* NH_4NO_3. Symbols as in Fig. 1.

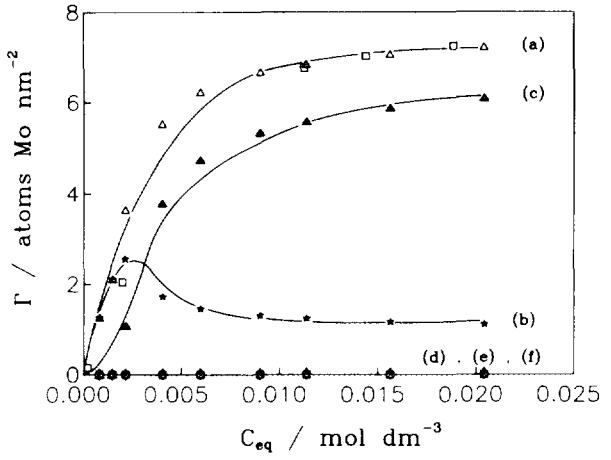

FIG. 8. Variation of the surface concentration of $Mo^{(VI)}$ with equilibrium $Mo^{(VI)}$ concentration. Deposition on pure γ-alumina, pH = 5.0, temperature = 50°C, ionic strength = 0.1 *M* NH_4NO_3. Symbols as in Fig. 1.

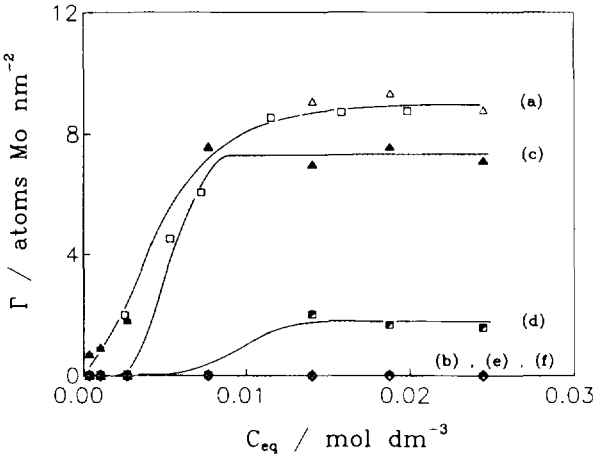

FIG. 10. Variation of the surface concentration of $Mo^{(VI)}$ with equilibrium $Mo^{(VI)}$ concentration. Deposition on sodium-doped γ-alumina [Na-*x*-γ-Al_2O_3]. pH = 5.0, temperature = 25°C, ionic strength = 0.1 *M* NH_4NO_3, *x* = 0.621 mmol Na g^{-1} Al_2O_3. Symbols as in Fig. 1.

based on the above considerations is illustrated in Fig. 16.

Effect of pH on the Various Parameters Calculated Using the Proposed Mechanistic Model (Figs. 1–5, Table 3)

Figures 1–5 clearly show considerable changes of the mode of the $Mo^{(VI)}$ deposition as pH increases. Thus, at pH = 4.1 (Fig. 1) the adsorption of the $Mo_7O_{24}^{6-}$ ions is predominant, whereas the extent of adsorption of MoO_4^{2-} ions is very small and the deposition of these ions by surface reaction with the neutral surface hydroxyls practically does not occur. As pH increased from 4.1 to 5 the extent of the whole Mo deposition decreased markedly in full agreement with the literature (e.g., Ref. (6)). This is mainly due to the decrease in the extent of adsorption of the $Mo_7O_{24}^{6-}$ ions which is now comparable (smaller), in the plateau (at low C_{eq} values), with (than) that obtained for the MoO_4^{2-} ions. Moreover, this increase in pH caused a slight increase in the amount of MoO_4^{2-} ions deposited by surface reaction. The above clearly show that, at pH values where the catalysts $Mo^{(VI)}$ species/γ-Al_2O_3 are usually prepared, the deposition of the molybdenum-oxo species actually takes place via adsorption (12–16). Moreover, the dramatic increase in the ratio adsorbed $Mo_7O_{24}^{6-}$/adsorbed MoO_4^{2-} and the increase in the extent of the whole deposition as pH decreased from 5 to 4.1 explains the increasing $Mo^{(VI)}$ polymerization and the decrease in the $Mo^{(VI)}$ species supported–support in-

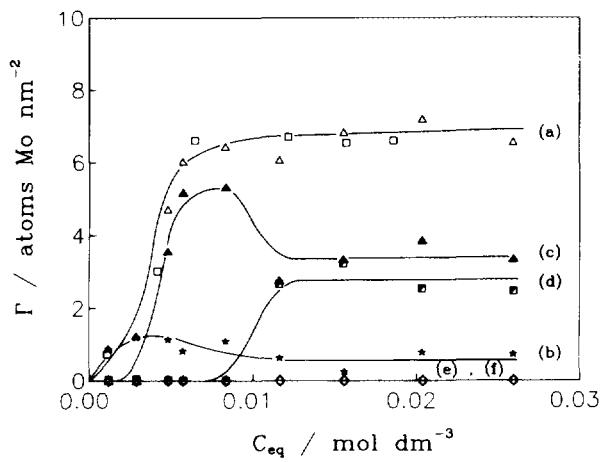

FIG. 9. Variation of the surface concentration of $Mo^{(VI)}$ with equilibrium $Mo^{(VI)}$ concentration. Deposition on sodium-doped γ-alumina [Na-*x*-γ-Al_2O_3]. pH = 5.0, temperature = 25°C, ionic strength = 0.1 *M* NH_4NO_3, *x* = 0.392 mmol Na g^{-1} Al_2O_3. Symbols as in Fig. 1.

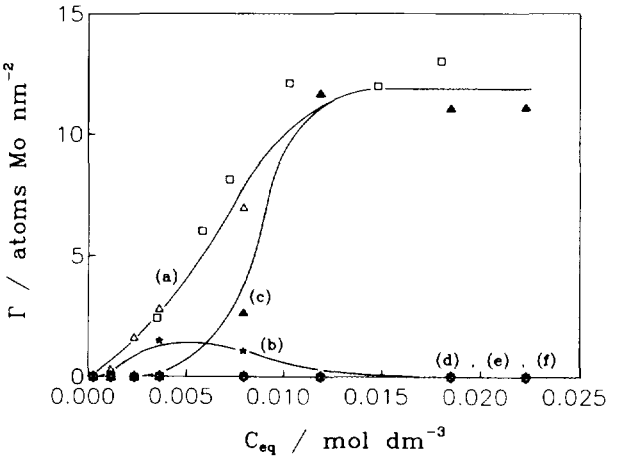

FIG. 11. Variation of the surface concentration of $Mo^{(VI)}$ with equilibrium $Mo^{(VI)}$ concentration. Deposition on sodium-doped γ-alumina [Na-*x*-γ-Al_2O_3]. pH = 5.0, temperature = 25°C, ionic strength = 0.1 *M* NH_4NO_3, *x* = 0.984 mmol Na g^{-1} Al_2O_3. Symbols as in Fig. 1.

TABLE 3

Effect of pH on the Various Parameters Calculated Using the Proposed Mechanistic Model

(1)	(2) K_1	(3) $K'_{f,5}$	(4) K_5	(5) $\frac{[MoO_4^{2-}]_b}{[Mo_7O_{24}^{6-}]_b}$	(6) $\frac{[MoO_4^{2-}]_{adsorb+react}}{[Mo_7O_{24}^{6-}]_{adsorb}}$	(7) $\frac{[MoO_4^{2-}]_{adsorb}}{[MoO_4^{2-}]_{react}}$	(8) $[AlOH]_t$	(9) $[AlOH_2^+]_t$	(10) $\frac{[OH]_t}{[OH_2^+]_t}$
pH									
4.1	74.1	3.5×10^{-17}	2208	1.2×10^{-1}	4.0×10^{-1}	2.1×10^{1}	8.9×10^{-4}	4.9×10^{-3}	1.8×10^{-1}
5.0	69.1	4.0×10^{-15}	4000	2.0×10^{0}	6.6×10^{0}	3.1×10^{0}	3.0×10^{-3}	2.7×10^{-3}	1.1×10^{0}
6.1	17.1	6.3×10^{-15}	40	2.2×10^{4}	1.3×10^{6}	1.0×10^{-2}	5.4×10^{-3}	1.9×10^{-4}	2.8×10^{1}
7.3	45.6	3.0×10^{-12}	75	2.1×10^{12}	5.0×10^{20}	1.6×10^{-3}	4.9×10^{-3}	4.7×10^{-5}	1.0×10^{2}
8.5	28.8	3.0×10^{-10}	30	2.0×10^{20}	2.2×10^{39}	3.4×10^{-5}	4.8×10^{-3}	2.1×10^{-5}	2.3×10^{2}
T (°C)									
35	60.2	1.0×10^{-15}	1000	2.0×10^{0}	3.7×10^{0}	5.4×10^{1}	2.1×10^{-3}	3.7×10^{-3}	5.6×10^{-1}
40	93.3	2.1×10^{-16}	210	2.0×10^{0}	4.0×10^{0}	5.8×10^{2}	1.6×10^{-3}	4.1×10^{-3}	3.9×10^{-1}
50	21.3	2.0×10^{-17}	20	2.0×10^{0}	2.6×10^{0}	8.0×10^{3}	1.1×10^{-3}	4.6×10^{-3}	2.4×10^{-1}
$\frac{\text{mmol Na}^+}{\text{g Al}_2\text{O}_3}$									
0.392	20.0	5.1×10^{-14}	5100	2.0×10^{0}	6.2×10^{0}	2.9×10^{-1}	2.4×10^{-3}	3.4×10^{-3}	7.0×10^{-1}
0.621	12.0	5.1×10^{-14}	5100	2.0×10^{0}	1.6×10^{0}	4.0×10^{-2}	2.0×10^{-3}	3.8×10^{-3}	5.0×10^{-1}
0.984	10.9	8.2×10^{-14}	8200	2.0×10^{0}	5.1×10^{-6}	7.6×10^{0}	1.8×10^{-6}	5.8×10^{-3}	2.9×10^{-4}
$\frac{\text{mmol Li}^+}{\text{g Al}_2\text{O}_3}$									
0.621	95.5	2.2×10^{-14}	2200	2.0×10^{0}	1.3×10^{1}	7.0×10^{-2}	2.4×10^{-3}	3.4×10^{-3}	7.0×10^{-1}
2.470	8.9	1.4×10^{-14}	1400	2.0×10^{0}	9.8×10^{0}	7.3×10^{-2}	1.7×10^{-3}	4.1×10^{-3}	4.1×10^{-1}

Note. Compilation of the conditional adsorption constants, K_1, $K'_{f,5}$, and K_5 corresponding to adsorption to positive (column 2) and neutral (columns 3, 4) sites, the concentration ratios of MoO_4^{2-} and $Mo_7O_{24}^{6-}$ ions in the bulk solution (column 5) and in the deposited state (column 6), the concentration ratio of MoO_4^{2-} ions adsorbed to positive and neutral sites (column 7), the concentration of the total neutral surface hydroxyls (column 8), the concentration of the total protonated surface hydroxyls (column 9) and the concentration ratio of the total neutral and protonated surface hydroxyls (column 10) at different conditions of pH (T = 25°C), temperature (pH = 5.0), and doping (pH = 5.0 and T = 25°C). In all cases the concentrations are expressed in mol dm^{-3} and correspond to the plateau of the respective isotherms.

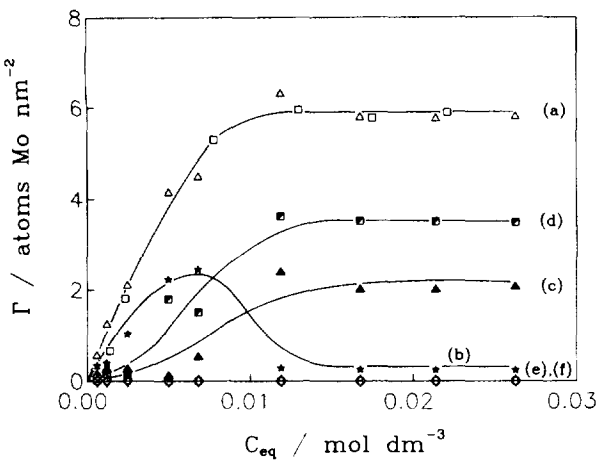

FIG. 12. Variation of the surface concentration of $Mo^{(VI)}$ with equilibrium $Mo^{(VI)}$ concentration. Deposition on lithium-doped γ-alumina [Li-x-γ-Al_2O_3]. pH = 5.0, temperature = 25°C, ionic strength = 0.1 M NH_4NO_3, x = 0.621 mmol Li g^{-1} Al_2O_3. Symbols as in Fig. 1.

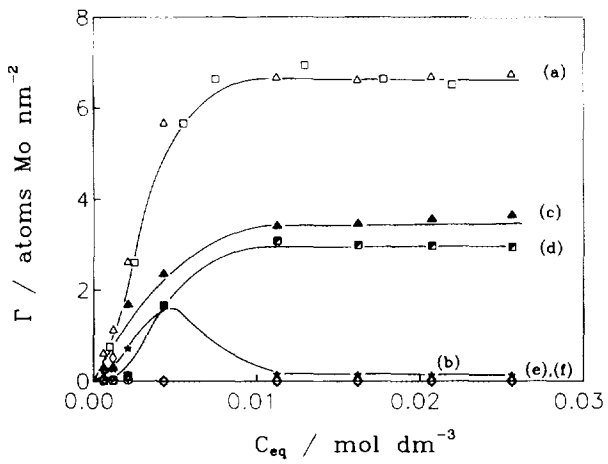

FIG. 13. Variation of the surface concentration of $Mo^{(VI)}$ with equilibrium $Mo^{(VI)}$ concentration. Deposition on lithium-doped γ-alumina [Li-x-γ-Al_2O_3]. pH = 5.0, temperature = 25°C, ionic strength = 0.1 M NH_4NO_3, x = 2.470 mmol Li g^{-1} Al_2O_3. Symbols as in Fig. 1.

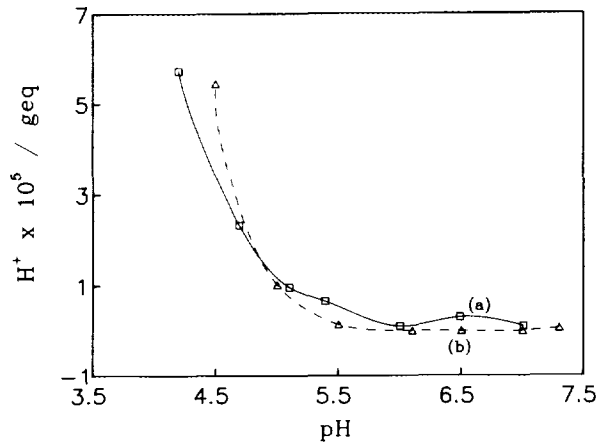

FIG. 14. Illustration of the variations, with pH, in the differences (in the presence and absence of molybdenum-oxo species) of the hydrogen consumed on the surface, $\Delta H^+_{consumed}$ (curve a), as well as of the "total protonated minus total deprotonated surface hydroxyls," $\Delta(AlOH_2^+ - AlO^-)_t$ (curve b). $\Delta H^+_{consumed}$ was determined experimentally, whereas $\Delta(AlOH_2^+ - AlO^-)_t$ was calculated using the proposed model. Pure support, T = 25°C, ionic strength = 0.1 M NH_4NO_3.

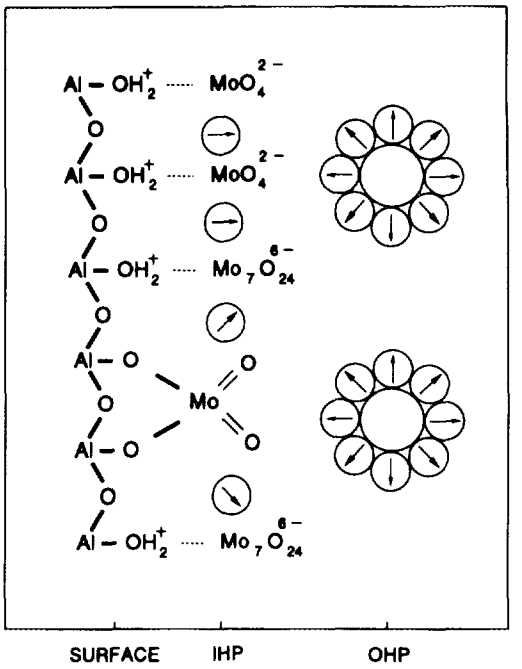

FIG. 16. Schematic representation of the deposition of the MoO_4^{2-} and $Mo_7O_{24}^{6-}$ ions on the γ-alumina surface.

teractions observed by us after calcination, in a recent work dealing with the characterization of the supported Mo phase of catalysts prepared by adsorption (34).

Further increase in pH from 5.0 to 6.1 caused a dramatic change in the mechanism of the Mo deposition. Although the form of the deposition isotherm (Fig. 3a, □ and △) could result in the conclusion that the adsorption remains the principal deposition mechanism (1, 6), it may be seen that at pH = 6.1 the $Mo^{(VI)}$ deposition practically occurs by the reaction of the MoO_4^{2-} with the neutral surface hydroxyls. Additional increase in pH from 6.1 to 8.5 does not change the deposition mechanism though it causes a progressive decrease in the extent of the aforementioned surface reaction and consequently in the whole Mo deposition (Figs. 3–5). From the above it can be concluded that the old view that the Mo deposition takes place via reaction (7–11) is correct only in the pH range 6.1–8.5,

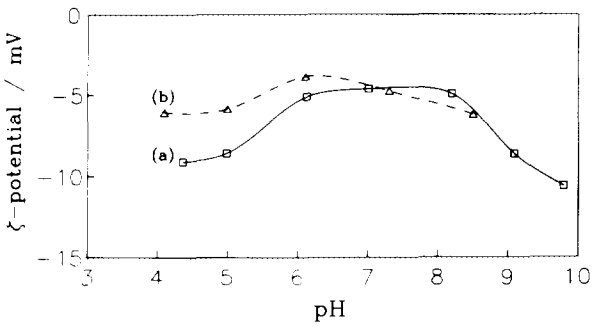

FIG. 15. Variation of the ζ-potential, with pH, in the presence of $Mo_xO_y^{z-}$ ions: (a) experimental values and (b) calculated values. Pure support, T = 25°C, ionic strength = 0.01 M NH_4NO_3.

where the catalysts $Mo^{(VI)}$ species/γ-alumina used industrially are rarely prepared due to their low Mo content. Moreover, the above allowed us to investigate the critical mechanistic point whether $Mo_7O_{24}^{6-}$ are dissociated into MoO_4^{2-} before adsorbing or whether they are adsorbed intact. Our results clearly show that in the pH range 4.1–5.0 the aforementioned oxopolyanions are adsorbed intact, whereas in the pH range 6.1–8.5 practically only MoO_4^{2-} ions are deposited by surface reaction. However, the fact that the molybdate ratio calculated in the bulk solution, "$[MoO_4^{2-}]_b/[Mo_7O_{24}^{6-}]_b$" (Table 3, column 5), is lower than the ratio "$[MoO_4^{2-}]_{absorb+react}/[Mo_7O_{24}^{6-}]_{adsorb}$" (Table 3, column 6) corroborates the finding previously reported (1, 6) that concerning deposition the selectivity of the support surface for the MoO_4^{2-} ions is higher than the selectivity for the $Mo_7O_{24}^{6-}$ ions.

The above-described effect of pH on the relative extent of the equilibria [1a], [1c], and [1e] may be interpreted in terms of the pH influence on both the composition of the molybdate solution and the surface features of γ-alumina. Concerning the composition of the molybdate solution the ratio $[MoO_4^{2-}]_b/[Mo_7O_{24}^{6-}]_b$ has been calculated in the bulk solution over the pH range studied. Table 3 (column 5) shows, in agreement with the literature and equilibrium [28], that this ratio increased markedly as pH increased. As to the γ-alumina surface it is expected, according to equilibria [32], that the total concentration of the protonated surface hydroxyls (which include both the free and bounded groups) should decrease as pH increases,

whereas the total concentration of the neutral hydroxyls is anticipated to pass from a maximum close to the point of zero charge (e.g., Ref. (3)). Table 3 (columns 8 and 9) shows that this is, in fact, the effect of pH in our case. The aforementioned variations in the protonated and neutral surface hydroxyls explain the increase in the ratio $[AlOH]_t/[AlOH_2^+]_t$ with pH (Table 3, column 10). This effect, in combination with the increase in the concentration of the negative surface hydroxyls as pH increased (see equilibria [32]), is expected to result in a decrease in the Ψ_1 and φ_0 values, which in turn should cause a decrease in the value of the adsorption constant $[K_1 = \exp\{(-\Delta G^\circ_{cs,1} + 2F\Psi_1 + F\varphi_0)/RT\}]$, in agreement with our results (Table 3, column 2). On the other hand, as pH increased, more and more $AlOH_2^+$ groups were deprotonated (see equilibrium [32a]) releasing neutral hydroxyls with increasing alkaline character. Therefore, a shift of the $\Delta G^\circ_{cs,5}$ to lower values is expected, which in turn causes an increase in the $K'_{f,5}$ $(K'_{f,5} = \exp(-\Delta G^\circ_{cs,5}/RT))$ with pH in full agreement with our results (Table 3, column 3). It is obvious that the increase in $K'_{f,5}$, the decrease in K_1, and the increase in the ratio $[AlOH]_t/[AlOH_2^+]_t$ with pH explain the decrease with pH of the ratio $[MoO_4^{2-}]_{adsorb}/[MoO_4^{2-}]_{react}$. This decrease in the values of the aforementioned ratio, determined for the plateau of the isotherms, is illustrated in Table 3 (column 7). Moreover, an increase in the ratio $[MoO_4^{2-}]_{adsorb+react}/[Mo_7O_{24}^{6-}]_{adsorb}$ with pH should be expected, even if the constant $K'_{f,5}$ and the ratio $[AlOH]_t/[AlOH_2^+]_t$ would remain unchanged, due to an analogous increase in the bulk ratio $[MoO_4^{2-}]_b/[Mo_7O_{24}^{6-}]_b$. The fact that $K'_{f,5}$ and $[AlOH]_t/[AlOH_2^+]_t$ increase with pH justifies the faster increase observed in the ratio of the molybdates in the deposited state compared with that observed in the bulk solution. This observation is an additional verification of the abovementioned finding stated in the first paper of this series that the adsorption of MoO_4^{2-} is favored with respect to the adsorption of $Mo_7O_{24}^{6-}$ (compare column 6 with column 5 of Table 3).

Effect of the Impregnation Temperature on the Various Parameters Calculated Using the Proposed Mechanistic Model (Figs. 2, 6–8, Table 3)

Figures 2 and 6–8 show that the increase in the impregnation temperature causes similar effects with those brought about by decreasing pH. An increase in the impregnating temperature caused a considerable increase in the extent of the whole Mo deposition which should mainly be attributed to the increase in the extent of adsorption of the $Mo_7O_{24}^{6-}$ ions, as the extent of adsorption of the MoO_4^{2-} ions did not change extensively and the deposition of these ions by surface reaction decreased. Thus, the ratio $[MoO_4^{2-}]_{adsorb+react}/[Mo_7O_{24}^{6-}]_{adsorb}$ determined at the plateau of the isotherms decreased from 6.6 (T = 25°C) to 2.6 (T = 50°C), whereas the corresponding ratio $[MoO_4^{2-}]_{adsorb}/[MoO_4^{2-}]_{react}$ increased from 3.1 (T = 25°C) to 8.0 × 10^3 (T = 50°C) (Table 3, columns 6 and 7). Since it has been presumed that equilibrium [28] does not shift substantially in the temperature range studied, a constant value was calculated for the ratio $[MoO_4^{2-}]_b/[Mo_7O_{24}^{6-}]_b$ in the whole temperature range (Table 3, column 5). Therefore, the changes of the Mo deposition should be attributed to the changes in the surface characteristics of the support caused by the increase in the impregnation temperature. Table 3 compiles the most important effects of the γ-alumina surface. The increase in $[AlOH_2^+]_t$ (column 9), the decrease in $[AlOH]_t$ (column 8), and therefore the decrease in the ratio $[AlOH]_t/[AlOH_2^+]_t$ (column 10) with the temperature should be anticipated due to the fact that equilibria [32a] and [32b] are exothermic and the former is more sensitive to the temperature changes than the latter (2). Moreover, Table 3 (column 3) shows that the increase in the impregnating temperature brings about a decrease in the values of $K'_{f,5}$. Equation [33], easily derived from Eq. [25], predicts a van't Hoff behaviour provided that the contribution of the chemical interactions between MoO_4^{2-} and AlOH to the standard enthalpy and entropy of equilibrium (1e), $\Delta H^\circ_{cs,5}$ and $\Delta S^\circ_{cs,5}$, does not change significantly with temperature.

$$\ln K'_{f,5} = -\Delta H^\circ_{cs,5}/RT + \Delta S^\circ_{cs,5}/R. \qquad [33]$$

The van't Hoff curve obtained (Fig. 17) demonstrates that this is the case. The calculated values $\Delta H^\circ_{cs,5} = -172.4$ kJ mol^{-1} and $\Delta S^\circ_{cs,5} = -0.851$ kJ mol^{-1} deg^{-1} seem to be reasonable. The above-described effects of temperature on the concentration of the surface hydroxyls and $K'_{f,5}$ explain the above-mentioned changes on the Mo deposition effortlessly. At this point it should be noted that the comparison of the molybdate ratio calculated in

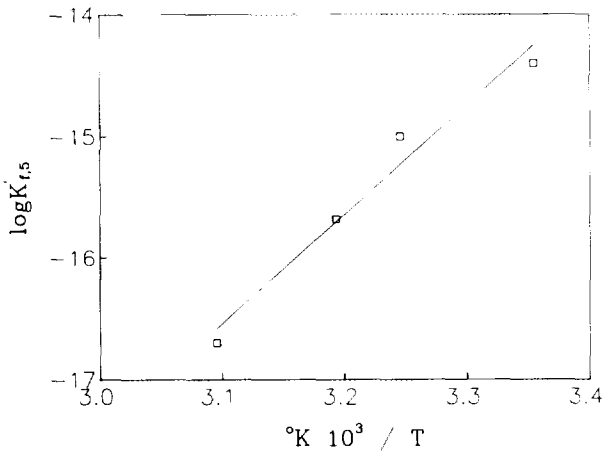

FIG. 17. Plot of Eq. [33].

the bulk solution (column 5) with the corresponding one calculated for the deposited state (column 6) confirms once again the finding previously reported (1, 6) that, concerning the deposition, the selectivity of the alumina surface for the MoO_4^{2-} ions is higher than the selectivity for the $Mo_7O_{24}^{6-}$ ions.

Finally, we shall discuss the influence of the impregnation temperature on the adsorption constant K_1. It can be observed that its value changes rather randomly with temperature (Table 3, column 2). An interpretation attempted is based on

$$\ln K_1 = -(\Delta H^\circ_{cs,1} + \Delta H^\circ_{elect,1})/RT + (\Delta S^\circ_{cs,1} + \Delta S^\circ_{elect,1}/R, \quad [34]$$

derived from Eq. [13], where $\Delta H^\circ_{cs,1}$, $\Delta H^\circ_{elect,1}$, $\Delta S^\circ_{cs,1}$, and $\Delta S^\circ_{elect,1}$ represent, respectively, the contribution to the standard enthalpy and entropy of adsorption of the adsorbate–adsorbent chemical and electrostatic interactions. Since the change in the impregnating temperature alters the relative concentration of the surface hydroxyls, it is expected to modify the surface charge of the support and thus the values of $\Delta H^\circ_{elect,1}$ and $\Delta S^\circ_{elect,1}$. Therefore, a linear dependence of $\ln K_1$ on the reciprocal of temperature should not be expected.

Effect of Doping on the Various Parameters Calculated Using the Proposed Mechanistic Model (Figs. 9–13, Table 3)

Although Na^+ or Li^+ doping increases considerably the amount of the deposited $Mo^{(VI)}$, the effects of this doping on the extent of equilibria [1a], [1c], and [1e] are not so simple compared with the corresponding effects of pH and temperature. Thus, inspection of Figs. 9–13 shows that the adsorption of the $Mo_7O_{24}^{6-}$ ions increased considerably due to the doping; the effect is more pronounced in the case of sodium. Moreover, it can be seen that the doping favours the deposition of the MoO_4^{2-} ions by reaction with the neutral surface hydroxyls, whereas the extent of these ions deposition by adsorption decreased slightly. These effects explain the decrease with doping in the ratio $[MoO_4^{2-}]_{adsorb}/[MoO_4^{2-}]_{react}$ determined at the plateau of the isotherms (column 7 of Table 3). Moreover, the ratio $[MoO_4^{2-}]_{adsorb+react}/[Mo_7O_{24}^{6-}]_{adsorb}$ decreased after Na^+ doping and increased after Li^+ doping (column 6 of Table 3) due to the fact that sodium doping increases $Mo_7O_{24}^{6-}$ adsorption more than MoO_4^{2-} deposition by reaction, whereas lithium doping increases $Mo_7O_{24}^{6-}$ adsorption less than MoO_4^{2-} deposition by reaction.

As the composition of the bulk solution is constant (Table 3, column 5), the above-mentioned effects on the $Mo_7O_{24}^{6-}$ and MoO_4^{2-} adsorption as well as on the MoO_4^{2-} deposition by surface reaction should be attributed to the modification of the support surface caused by the doping. Inspection of Table 3 (columns 8–10) shows, in agreement with the literature (4, 5), that the Na^+ or Li^+ doping increased the concentration of the protonated surface hydroxyls and decreased the concentration of the neutral surface hydroxyls, thus decreasing the ratio $[AlOH]_t/[AlOH_2^+]_t$. The increase in the $[AlOH_2^+]_t$ and therefore in the adsorption sites, due to the doping, overcompensates the decrease in the adsorption constant, K_1 (Table 3, column 2), bringing about an increase in the amount of the $Mo_7O_{24}^{6-}$ and MoO_4^{2-} ions deposited by adsorption. On the other hand the increase in the values of the reaction constant, $K'_{f,5}$, (Table 3, column 3) seems to overbalance the decrease in the concentration of the neutral surface hydroxyls resulting in the enhancement of the MoO_4^{2-} deposition through surface reaction.

As to the above-mentioned decrease in K_1, this should be related with an increase in $\Delta G^\circ_{cs,1}$ which seems to overbalance the anticipated decrease in the $\Delta G^\circ_{elect,1} = -F(2\Psi_1 + \varphi_0)$ caused by the increase in the concentration of the protonated surface hydroxyls. Two additional observations about the values of K_1 and $K'_{f,5}$ are notable. First, the increase in the value of $K'_{f,5}$ is observed after the doping with the minimum amount of the dopant ions. The second observation refers to all K_1 and $K'_{f,5}$ values calculated in the present work. Inspection of columns 2 and 3 of Table 3 shows that in all cases the values of K_1 are much higher than the corresponding values of $K'_{f,5}$. This indicates that the ionic bond formed between protonated surface hydroxyls and the specifically adsorbed MoO_4^{2-} and $Mo_7O_{24}^{6-}$ ions is much stronger than the covalent bond Al–O–Mo formed in the surface complex illustrated in equilibrium [1e]. This may be explained by taking into account that the adsorbed Mo species are located very close to the surface and thus the coulombic attraction, depending on $1/r^2$, should be very strong.

CONCLUSIONS

The following conclusions may be drawn from the present work.

(i) The deposition of the $Mo^{(VI)}$ species on the γ-alumina surface takes place by adsorption of $Mo_7O_{24}^{6-}$ and MoO_4^{2-} ions on sites created by the protonated surface hydroxyls of the support in the IHP of the double layer developed between the surface of the support particles and the impregnating solution. Each protonated surface hydroxyl creates one adsorption site.

(ii) Moreover, the aforementioned deposition takes place through reaction of each MoO_4^{2-} ion with two neu-

tral surface hydroxyls resulting in the formation of the surface complex

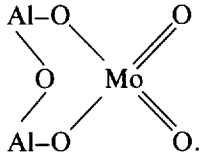

(iii) Strong lateral interactions are exerted between the deposited Mo species, mainly between the adsorbed MoO_4^{2-} and $Mo_7O_{24}^{6-}$ ions through water molecules located at the IHP.

(iv) A comparison of the equilibrium constants calculated for the adsorption of $Mo_7O_{24}^{6-}$ and MoO_4^{2-} ions as well as for the deposition by reaction of the MoO_4^{2-} ions demonstrated that the ionic sorptive bond is much stronger than the covalent Al–O–Mo bond in the above-illustrated surface complex.

(v) A decrease in pH of the impregnating solution from 8.5 to 4.1 caused the following effects: (a) The amount of the deposited $Mo^{(VI)}$ species increases. (b) The extent of adsorption increases and the extent of deposition by reaction decreases. Thus, in the pH range 8.5–6.1 the deposition takes place practically by reaction, whereas in the pH range 6.1–4.1, where the $Mo^{(VI)}$ species/γ-alumina catalysts are usually prepared, the Mo deposition predominates via adsorption. (c) The amount of the adsorbed $Mo_7O_{24}^{6-}$ increases at the expense of the amount of the deposited MoO_4^{2-}. (d) The above phenomena were explained on the basis of the effects which were caused by the decrease in pH on both the composition of the bulk solution (decrease in the ratio $[MoO_4^{2-}]_b/[Mo_7O_{24}^{6-}]_b$) and the γ-alumina surface (increase in the concentration of the protonated surface hydroxyls, increase in the values of the adsorption constant, decrease in the value of the reaction constant). (e) The influence of pH on the above-mentioned surface parameters may be explained by the protonation–deprotonation equilibria of this support and by the equations derived from the proposed mechanism for the Mo deposition.

(vi) Increasing the impregnating temperature from 25 to 50°C at pH = 5 caused effects similar to those brought about by decreasing pH. That is a considerable increase in the extent of the whole Mo deposition which should mainly be attributed to the increase in the extent of the $Mo_7O_{24}^{6-}$ ion adsorption, as the extent of the MoO_4^{2-} ion adsorption did not change considerably and the deposition of these ions by surface reaction decreased. The above were explained by taking into account the effects, which were caused by the increase in the impregnation temperature, on several surface parameters (increase in the concentration of the protonated surface hydroxyls, decrease in the concentration of the neutral surface hydroxyls, and decrease in the equilibrium constant for the deposition of the MoO_4^{2-} ions through surface reaction).

(vii) Na^+ and Li^+ doping increases considerably the amount of the deposited Mo which should mainly be attributed to the increase in the extent of the $Mo_7O_{24}^{6-}$ ion adsorption as well as to the increase in the extent of deposition by reaction of the MoO_4^{2-} ions. The increase in the extent of the $Mo_7O_{24}^{6-}$ ion adsorption was attributed to the increase in the concentration of the protonated surface hydroxyls, which overcompensates the decrease in the adsorption constant. Whereas the increase in the extent of the MoO_4^{2-} ion deposition through reaction with the neutral surface hydroxyls was attributed to the increase in the reaction constant which overbalances the decrease in the concentration of these hydroxyls.

(viii) The ratio $[MoO_4^{2-}]_b/[Mo_7O_{24}^{6-}]_b$ calculated in the bulk solution was always lower than the ratio $[MoO_4^{2-}]_{adsorb+react}/[Mo_7O_{24}^{6-}]_{adsorb}$ calculated in the deposited state, corroborating a previous finding that, concerning deposition, the selectivity of the support surface for the MoO_4^{2-} ions is higher than the selectivity for the $Mo_7O_{24}^{6-}$ ions.

ACKNOWLEDGMENT

We gratefully acknowledge kind help given by Professor P. G. Koutsoukos in the application of the computer program SURFEQL.

REFERENCES

1. Spanos, N., Vordonis, L., Kordulis, Ch., and Lycourghiotis, A., *J. Catal.* **124,** 301 (1990).
2. Akratopulu, K., Vordonis, L., and Lycourghiotis, A., *J. Chem. Soc., Faraday Trans. 1* **82,** 3697 (1986).
3. Vordonis, L., Koutsoukos, P. G., and Lycourghiotis, A., *J. Chem. Soc., Chem. Commun.*, 1309 (1984).
4. Vordonis, L., Koutsoukos, P. G., and Lycourghiotis, A., *J. Catal.* **98,** 296 (1986).
5. Vordonis, L., Koutsoukos, P. G., and Lycourghiotis, A., *J. Catal.* **101,** 186 (1986).
6. Spanos, N., Vordonis, L., Kordulis, Ch., Koutsoukos, P. G., and Lycourghiotis, A., *J. Catal.* **124,** 315 (1990).
7. Iannibello, A., Marengo, S., Trifiro, F., and Villa, P. L., *in* "2nd International Symposium on Scientific Basis for the Preparation of Heterogeneous Catalysts." Louvain La Neuve, Belgium, 1978.
8. Van Veen, J. A. R., De Wit, Emeis, C. A., and Hendriks, P. A. J. M., *J. Catal.* **107,** 579 (1987).
9. Iannibello, A., and Mitchell, P.C . H., in "2nd International Symposium on Scientific Basis for the Preparation of Heterogeneous Catalysts." Louvain La Neuve, Belgium, 1978.
10. Van Veen, J. A. R., and Hendriks, P. A. J. M., *Polyhedron* 5, 75 (1986).
11. Jeziorowski, H., and Knozinger, H., *J. Phys. Chem.* **83,** 1166 (1979).
12. Wang, L., and Hall, W. K., *J. Catal.* **77,** 232 (1982).
13. Kasztelan, S., Grimblot, J., Bonnelle, J. P., Payen, E., Toulhoat, H., and Jacquin, Y., *Appl. Catal.* **7,** 91 (1983).
14. Caceres, C. V., Fierro, L. G., Agudo, A. L., Blanco, M. N., and Thomas, H. J., *J. Catal.* **95,** 501 (1985).
15. Houalla, M., Kibby, C. L., Petrakis, L., and Hercules, D. M., *J. Catal.* **83,** 50 (1983).
16. Luthra, N. P., and Cheng, W. C., *J. Catal.* **107,** 154 (1987).

17. Knozinger, H., and Jeziorowski, H., *J. Phys. Chem.* **82,** 2002 (1978).
18. Medema, J., van Stam, C., de Beer, V.H. J., Konings, A. J. A., and Koningsberger, D. C., *J. Catal.* **53,** 386 (1978).
19. Sonnemans, J., and Mars, P., *J. Catal.* **31,** 209 (1973).
20. Wang, L., and Hall, W. K., *J. Catal.* **66,** 251 (1980).
21. Wang, L., and Hall, W. K., *J. Catal.* **83,** 242 (1983).
22. Mulcahy, F. M., Fay, M. J., Proctor, A., Houalla, M., Hercules, D. M., *J. Catal.* **124,** 231 (1990).
23. Faughnan, J. "SURFEQL An Interactive Code for the Calculation of Chemical Equilibria in Aqueous Systems." W. M. Keck Laboratories 138-78, California Institute of Technology, Pasadena, California 91125.
24. Davis, J. A., and Leckie, J. O., *J. Colloid Interface Sci.* **74,** 32 (1980).
25. de Keizer, A., and Lyklema, J., *J. Colloid Interface Sci.* **75,** 171 (1980).
26. Hough, D. B., and Rendall, H. M., *in* "Adsorption from Solution at the Solid/Liquid Interface," Chap. 6 (G. D. Parfitt and C. H. Rochester, Eds.), Academic Press, London, 1983.
27. Jaycock, M. J., and Parfitt, G. D., "Chemistry of Interfaces", Wiley, New York, 1981.
28. Smith, R. M., and Martell, A. E., *in* "Critical Stability Constants," Vol. 4. Plenum, New York, 1981.
29. Sprycha, R., *J. Colloid Interface Sci.* **96,** 551 (1983).
30. Huang, C. P., "The Chemistry of the Aluminum Oxide-Electrolyte Interface." Ph. D. Thesis, Harvard University, 1971.
31. Spanos, N., Matralis, H. K., Kordulis, Ch., and Lycourghiotis, A., *J. Catal.* **136,** 432 (1992).
32. Vordonis, L., Spanos, N., Koutsoukos, P. G., and Lycourghiotis, A., *Langmuir* **8,** 1736 (1992).
33. Karakonstantis, L., Kordulis, Ch., and Lycourghiotis, A., *Langmuir* **8,** 1318 (1992).
34. Spanos, N., Kordulis, Ch., and Lycourghiotis, A., in preparation.